



Published in final edited form as:

J Mol Cell Cardiol. 2010 July ; 49(1): 5–15. doi:10.1016/j.yjmcc.2010.02.007.

Evidence for a Role of Immunoproteasomes in Regulating Cardiac Muscle Mass in Diabetic Mice

Lingyun Zu^{a,b}, Djahida Bedja^c, Karen Fox-Talbot^d, Kathleen L. Gabrielson^c, Luc Van Kaer^e, Lewis C. Becker^a, and Zheqing P. Cai^{a,*}

^a Division of Cardiology, Department of Medicine, Johns Hopkins University School of Medicine, Baltimore, MD 21205, USA

^b Department of Cardiology, Peking University Third Hospital, Beijing 100191, China

^c Division of Comparative Medicine, Johns Hopkins Medical Institutions, Baltimore, MD21205, USA

^d Department of Pathology, Johns Hopkins University School of Medicine, Baltimore, MD 21205, USA

^e Department of Microbiology and Immunology, Vanderbilt University School of Medicine, Nashville, TN37232, USA

Abstract

The ubiquitin-proteasome system plays an important role in regulating muscle mass. Inducible immunoproteasome subunits LMP-2 and LMP-7 are constitutively expressed in the heart; however, their regulation and functions are poorly understood. We here investigated the hypothesis that immunoproteasomes regulate cardiac muscle mass in diabetic mice. Type 1 diabetes was induced in wildtype mice by streptozotocin. After hyperglycemia developed, insulin and the proteasome inhibitor epoxomicin were used to treat diabetic mice for 6 weeks. Isolated mouse hearts were perfused with control or high glucose solution. Catalytic proteasome β -subunits and proteolytic activities were analyzed in the heart by immunoblotting and fluorogenic peptide degradation assays, respectively. Insulin and epoxomicin blocked loss of heart weight and improved cardiac function in diabetic mice. LMP-7 and its corresponding chymotryptic-like proteasome activity were increased in diabetic hearts and high glucose-treated hearts. Myosin heavy chain protein was decreased in diabetic hearts, which was largely reversed by epoxomicin. High glucose decreased LMP-2 protein levels in perfused hearts. In diabetic hearts, LMP-2 expression was downregulated whereas expression of the phosphatase and tensin homologue deleted on chromosome ten (PTEN) and the muscle atrophy F-box were upregulated. Moreover, mice with muscle-specific knockout of PTEN gene demonstrated increased cardiac muscle mass, while mice with LMP-2 deficiency demonstrated PTEN accumulation, muscle mass loss, and contractile impairment in the heart. Therefore, we concluded that high glucose regulates immunoproteasome subunits and modifies proteasome activities in the heart, and that dysregulated immunoproteasome subunits may mediate loss of cardiac muscle mass in experimental diabetic mice.

*Corresponding author: Dr. Zheqing P. Cai, 720 Rutland Avenue, Ross 333, Baltimore, MD 21205, USA. Telephone: 410-502-5985. Fax: 410-502-1975. czheqin1@jhmi.edu.

No conflicts of interest relevant to this article were reported.

Publisher's Disclaimer: This is a PDF file of an unedited manuscript that has been accepted for publication. As a service to our customers we are providing this early version of the manuscript. The manuscript will undergo copyediting, typesetting, and review of the resulting proof before it is published in its final citable form. Please note that during the production process errors may be discovered which could affect the content, and all legal disclaimers that apply to the journal pertain.

Keywords

Proteasome; PTEN; cardiomyopathy; heart failure; hyperglycemia

1. Introduction

Diabetes mellitus is an independent risk factor for heart failure [1,2]. The pathological changes in diabetic hearts are characterized by loss of cardiac muscle mass and deposition of connective tissue [3,4]. The loss of contractile components contributes to cardiac dysfunction. The ubiquitin-proteasome system (UPS) has been shown to mediate loss of muscle mass, including cardiac muscle mass, in type 1 diabetes [5–7]. However, the underlying molecular mechanism is not fully understood.

UPS controls protein quantity and quality [8]. The 26S proteasome is composed of regulatory 19S and catalytic 20S components [9–12]. The 20S proteasome possesses four stacked rings, with two outer rings containing seven different α subunits and the two inner rings containing seven different β subunits. The proteasome has three catalytic β subunits ($\beta 1$, $\beta 2$, and $\beta 5$) that are constitutively expressed, but they can be replaced by inducible β subunits to form so-called immunoproteasomes. Constitutive β subunits are relatively stable in the heart and liver compared to inducible β subunits [12]. Inducible β subunits are abundantly expressed in the heart under basal conditions and mediate proteolytic activities [11,12]. However, little is known about their regulation and functions in the heart. Inducible β subunits, consisting of low molecular mass polypeptide (LMP)-2/ $\beta 1i$, multicatalytic endopeptidase complex-like (MECL)-1/ $\beta 2i$, and LMP-7/ $\beta 5i$, preferentially form immunoproteasomes [13]. LMP-2 is required for the incorporation of MECL-1. LMP-7, together with the constitutive $\beta 5$ subunit, mediates the chymotryptic-like activity of 20S proteasomes [12]. Originally, the immunoproteasome subunits were regarded as transiently induced subunits to promote antigenic peptide production in response to inflammatory stimuli by modifying the specificity and activities of 20S proteasomes [13]. However, recent studies have shown that LMP-2 and LMP-7 modify proteasome activities and increased cell survival under non-inflammatory conditions [11,14].

Myocyte size and survival are negatively regulated by the phosphatase and tensin homologue deleted on chromosome ten (PTEN) [15]. Protein kinase B (also called Akt), an important downstream protein of PTEN, has been shown to increase muscle mass by inactivating forkhead box class O transcription factor (FOXO) 3a [16,17]. In the present study, we have demonstrated that high glucose regulates immunoproteasome subunits and proteolytic activities of proteasomes, and that immunoproteasome dysregulation may mediate loss of cardiac muscle mass in diabetic mice.

2. Materials and methods

2.1. Animals

All experiments were performed with age-matched male mice. At the time of the experiments, mice were at least 2 months old. *Lmp-2* knockout (*Lmp-2*^{-/-}) mice were generated by deletion of the corresponding gene using embryonic stem cell technology [18]. *Lmp-2*^{-/-} mice were backcrossed 10 times to C57BL6. B6.129S4-*Pten*^{tm1Hwu}/*J* mice and B6.129S4-*Tg(ckm-cre)* 5*Kh*n/*J* mice were purchased from The Jackson Laboratory. All procedures were approved by the Johns Hopkins University Institutional Animal Care and Use Committee and conformed to the Guide for the Care and Use of Laboratory Animals published by the U.S. National Institutes of Health (NIH Publication No. 85-23, revised 1996).

2.2. Generation of muscle-specific *Pten* knockout mice

Muscle-specific *Pten* knockout mice were generated from B6.129S4-*Pten*^{tm1Hwu/J} (*Pten*^{l^p/l^p}) mice and B6.129S4-*Tg(ckm-cre)5Khn/J* (*mck-Cre*^{+/-}) mice. *Pten*^{l^p/l^p} mice possess two flanked loxp sites on either side of exon 5 of the *Pten* gene. In *mck-Cre*^{+/-} mice, the Cre recombinase transgene is driven by the muscle creatine kinase (mck) promoter. *Pten*^{l^p/l^p} mice were crossed with *mck-Cre*^{+/-} mice and their offspring were backcrossed to *Pten*^{l^p/l^p} mice. *Pten*^{l^p/l^p}; *mck-Cre*^{+/-} mice were identified by genotyping (the protocols were provided by The Jackson Laboratory). PTEN deletion in cardiac muscle was confirmed by immunohistochemistry and Western blot analysis. *Pten*^{l^p/l^p}; *mck-Cre*^{-/-} mice were used as controls.

2.3. Protocols for animal experiments

Diabetes was induced in mice by intra-peritoneal injection of STZ (two doses at 150 mg/kg, one day apart). STZ was dissolved in PBS. Hyperglycemia developed within one week. Diabetic mice were divided into three groups. The first group was given PBS. The second group received insulin replacement by a daily sc injection of Lantus (Sanofi-Aventis, Bridgewater, NJ, USA) at 8 U/100 g body weight, starting on the third day after STZ injection. The third group was treated with the specific and irreversible proteasome inhibitor epoxomicin (EPX) (Biomol International, Plymouth Meeting, PA, USA) for six weeks (0.5 mg/kg ip, once a week). As previously reported, EPX inhibited proteasome activity [19]. Normal wildtype mice treated with EPX were used as a control group. The mice tolerated this dosage of EPX without obvious side effects. At the end of the experiments, echocardiography was performed, and blood glucose and body weight were measured. Left ventricular function was assessed by a Mikro-tip pressure catheter, and then the heart was removed and cross-sectioned into 5 pieces. Cardiac sections were stained by 1.5% triphenyltetrazolium chloride (TTC) for 15 min at 37 °C. The heart and individual sections were weighed and photographed. Left ventricular muscle mass (LVM, red) was measured by computerized planimetry (Image J, NIH, Bethesda, MD) using the following equation: LVM = heart weight × LV muscle area (red)/[muscle area (red) + fibrosis area (white)]. Tibial length was measured, and the ratio of heart weight to tibial length was calculated.

2.4. Immunohistochemistry

Formalin-fixed, paraffin-embedded hearts were sectioned at 6 μm, as described previously [20]. Briefly, sections were deparaffinized, and then heat-induced antigen retrieval was performed by Trilogy EDTA (Cell Marque Corp.), followed by a hot rinse in Trilogy. Endogenous peroxidase activity was blocked by incubation in 0.3% H₂O₂. Slides were incubated with anti-PTEN antibody (Cell Signaling Technology) for 3 hours. Sections were counterstained in hematoxylin.

2.5. Mouse Langendorff preparation

Mice were anesthetized by intraperitoneal injection of pentobarbital (70 mg/kg), as described previously [11]. Hearts were removed and perfused at a constant pressure with modified Krebs-Henseleit (KH) buffer (in mmol/L: glucose 16.5, NaCl 120, NaHCO₃ 25, CaCl₂ 2.5, KCl 5.9, MgSO₄ 1.2, and EDTA 0.5), which was maintained at 37°C and bubbled continuously with a mixture of 95% O₂ and 5% CO₂. Perfusion with high glucose was achieved by increasing the glucose concentration in the perfusate from 16.5 mmol/L to 33.0 mmol/L, without changes in the other components.

2.6. Measurement of proteolytic activities of 20S proteasomes

Proteolytic activities of 20S proteasomes were measured by fluorogenic peptide degradation assays, as described previously [11,12]. Briefly, hearts were homogenized on ice in the assay buffer (25 mmol/L HEPES, pH 7.5, 0.5 mmol/L EDTA, 0.03% SDS). Equal amounts of protein

were reacted with 0, 10, or 50 $\mu\text{mol/L}$ of the substrates at room temperature. Suc-LLVY-aminomethylcoumarin (-AMC) and Z-LLE-AMC were used to measure chymotryptic-like and caspase-like proteasome activity, respectively. Boc-LLR-AMC was used to measure tryptic-like proteasome activity in a separate buffer (25 mmol/L HEPES, pH 7.5, 0.5 mmol/L EDTA, 0.05% NP-40, 0.001% SDS). The cleavage product AMC was analyzed in a fluorometer (excitation/emission: 355/460 nm). Background activity (caused by nonproteasomal degradation) was determined by addition of the proteasome inhibitor lactacystin at a final concentration of 50 $\mu\text{mol/L}$. Lactacystin and all proteasome substrates were purchased from Biomol International, Plymouth Meeting, PA, USA.

2.7. Echocardiography

In vivo cardiac function was assessed by transthoracic echocardiography (Acuson Sequoia C256, 13MHz transducer; Siemens) in conscious mice, as described previously [21]. M-mode LV end-systolic and end-diastolic dimensions were averaged from 3–5 beats. Fractional shortening (FS) was calculated from the end-diastolic diameter (EDD) and end-systolic diameter (ESD) using the following equation: $\text{FS} = 100\% \times [(\text{EDD} - \text{ESD})/\text{EDD}]$. Studies and analysis were performed by investigators blinded to genotype or treatments.

2.8. Measurement of left ventricular pressure

After mice were anesthetized with pentobarbital (70 mg/kg) and were mechanically ventilated, a Mikro-tip catheter (SPR671, Millar Instruments, Houston, Texas, USA) was inserted into the left ventricle as we described previously [11]. Left ventricular pressure was directly measured with the Powerlab Data Acquisition System and displayed on a computer. Left ventricular developed pressure [LVDP = systolic pressure (LVSP) – end diastolic pressure (LVEDP)], heart rate (HR), positive maximal LVP derivative ($+\text{dp}/\text{dt}_m$), and negative maximal LVP derivative ($-\text{dp}/\text{dt}_m$) were automatically calculated using Chart 5 software (ADInstruments, Colorado Springs, Colorado, USA).

2.9. Immunoblotting assay

Hearts were homogenized in the lysate buffer (in mmol/L: pH 7.5 Tris 20, NaCl 150, EDTA 1, EGTA 1, PMSF 1, Na_3VO_4 1, 1% Triton). Proteins were separated on a precast NuPAGE Bis-Tris gel (Invitrogen) and transferred to a nitrocellulose membrane. Proteins were detected by using primary antibodies, followed by horseradish peroxidase-conjugated secondary antibody and enhanced chemiluminescence. Antibodies against PTEN, p-Akt (S-473), Akt, p-FOXO3a, FOXO3a, and GAPDH were purchased from Cell Signaling Technology. MAFbx antibody was from Santa Cruz Biotechnology. Antibodies against LMP-2, MHC, and MyoD1 were from Abcam Inc. Antibodies against LMP-7, MECL-1, $\beta 1$, $\beta 2$, $\beta 5$, and $\alpha 5$ subunit were from Biomol International, Plymouth Meeting, PA, USA.

2.10. Statistical analysis

Data are presented as mean \pm standard error of the mean. The difference among groups was analyzed by one-way ANOVA or Student's t-test. Differences were considered significant if $p < 0.05$.

3. RESULTS

3.1. Diabetic cardiomyopathy in STZ-treated mice is attenuated by proteasome inhibition

After 6 weeks of diabetes, STZ-treated mice exhibited lower body weight (BW) and heart weight (HW) than control (CON) mice (Table 1). Moreover, the study of left ventricular function showed that LVDP, $+\text{dp}/\text{dt}$, $-\text{dp}/\text{dt}$, and FS were significantly decreased in STZ-treated mice. Insulin replacement controlled blood glucose, inhibited the loss of BW and HW,

and improved the left ventricular systolic function (Table 1 and Fig. 1). Therefore, diabetic cardiomyopathy was present in STZ-treated mice. However, LVEDP was unchanged in STZ-treated mice. To determine whether 20S proteasomes play a role in diabetic cardiomyopathy, we treated diabetic mice with EPX for 6 weeks. EPX did not decrease blood glucose in STZ mice, but it significantly increased BW and HW and improved LVDP, +dp/dt, -dp/dt, and FS in these diabetic mice. EPX itself did not increase HW and FS but instead decreased the ratio of HW/BW (Table 1 and Fig. 1). Taken together, these results suggested that 20S proteasomes play an important role in the development of diabetic cardiomyopathy.

3.2. High glucose increases LMP-7 protein levels and its *corresponding* chymotryptic-like proteasome activity in the heart

To determine whether LMP-7 and $\beta 5$ subunit are regulated in STZ-treated mice, we measured them by Western blot analysis. LMP-7 and $\beta 5$ subunit protein levels were increased in STZ hearts by 280% and 82%, respectively (Fig. 2A). However, non-catalytic $\alpha 5$ subunit was unchanged (Fig. S1A). To determine whether high glucose regulates LMP-7 and $\beta 5$ subunit in the heart, we exposed isolated hearts from wildtype mice to high glucose (HG) or the perfusion buffer containing control glucose (CG) for 4 hrs. HG significantly increased LMP-7 protein levels (Fig. 2A). However, $\beta 5$ subunit protein levels were unchanged in HG-treated hearts (Fig. 2A). To determine whether STZ directly regulates LMP-7 in the heart, we exposed isolated mouse hearts to different concentrations of STZ for 4 hrs. LMP-7 protein levels were not increased in the STZ-treated hearts (Fig. S2). Moreover, to determine whether LMP-7 upregulation in the heart is caused by high osmotic pressure, we subjected isolated mouse hearts to HG or mannitol perfusion buffer for 4 hrs. The two buffers were equal in osmotic pressure. HG increased LMP-7 protein levels, but mannitol did not (Fig. S3). Consistent with the increase in LMP-7, the chymotryptic-like proteasome activity was also significantly increased in diabetic hearts (Fig. 2B) and in HG hearts (Fig. 2B).

3.3. MHC protein levels are reduced in hearts from STZ-treated mice through the proteasome pathway

To determine whether increased proteasome activity regulates MHC protein levels in hearts from STZ-treated mice, we treated diabetic mice with or without the proteasome inhibitor epoxomicin. MHC was significantly decreased in diabetic mice (Fig. 3A). However, epoxomicin blocked the proteasome-mediated downregulation of MHC by 75% (Fig. 3A). No difference in MHC protein levels was found in diabetic mice treated with EPX treatment and insulin treatment. Moreover, MHC protein levels were not increased in EPX-treated normal mice (Fig. 3B). Therefore, increased proteasome activity mediates loss of MHC protein, most likely through its degradation, in diabetic hearts.

3.4. High glucose decreases LMP-2 protein levels in the heart

LMP-2 is essential for the formation of immunoproteasomes [11,13]. To determine whether LMP-2 is regulated in diabetic hearts, we measured LMP-2 levels in control and STZ hearts. LMP-2 was significantly decreased in diabetic mice (Fig. 4A). Next, we analyzed $\beta 1$, MECL-1, and $\beta 2$ subunits in these samples. A modest increase in $\beta 1$ was found in STZ hearts (Fig. 4A). MECL-1 was significantly decreased in STZ hearts (Fig. 4A), but no significant change was found in $\beta 2$ protein. To determine whether high glucose regulates LMP-2 in the heart, we measured LMP-2 protein levels in isolated mouse hearts perfused with HG. HG significantly decreased LMP-2 levels in the heart (Fig. 4A), but had no effect on $\beta 1$ subunit, MECL-1, and $\beta 2$ subunit (Fig. 4A). After isolated hearts were exposed to mannitol perfusion buffer for 4 hrs, no decrease in LMP-2 and MECL-1 was found (Fig. S2). Moreover, direct exposure of isolated hearts to STZ did not cause a decrease in LMP-2 and MECL-1 (Fig. S2). To assess whether the alteration in LMP-2 levels impacts the proteolytic activities of proteasomes, we measured

caspase-like and tryptic-like proteasome activity in CON and STZ hearts. Tryptic-like proteasome activity was significantly decreased in diabetic hearts (Fig. 4B). However, no significant change was found in caspase-like proteasome activity between these groups.

3.5. PTEN accumulation and MAFbx expression are increased in STZ-induced diabetic hearts

To determine whether the signaling pathway for muscle degradation is activated in diabetic hearts, we first determined the effect of LMP-2 downregulation on PTEN protein levels in diabetic hearts. PTEN protein levels were significantly increased in hearts from STZ-treated mice (Fig. 5). We then measured p-Akt and total Akt, p-FOXO3a and total FOXO3a, MAFbx, and MyoD1 in STZ and CON hearts. p-Akt was significantly decreased in diabetic hearts (Fig. 5). The levels of total Akt were also decreased, but the ratio of p-Akt to total Akt remained significantly decreased in these hearts (17 ± 7 vs. 73 ± 3 %). Consistent with these results, p-FOXO3a was significantly decreased (Fig. 5), and MAFbx was significantly increased (Fig. 5). Moreover, the myogenic regulatory factor MyoD1 was decreased in diabetic hearts (Fig. 5). However, Erk1/2 phosphorylation was not significantly different in STZ and CON hearts (Fig. S1B). Taken together, these results suggested that PTEN activity is increased and that signaling for muscle-specific protein degradation may be up-regulated in STZ-induced diabetic hearts.

3.6. PTEN inactivation increases cardiac muscle mass in mice

To demonstrate that PTEN regulates cardiac muscle mass in mice, we generated muscle-specific *Pten* knockout mice (*Pten*^{l^p/l^p; *mck-Cre*^{+/-} mice). We detected PTEN protein levels in the heart by immunohistochemistry. *Pten*^{l^p/l^p; *mck-Cre*^{-/-} mice were used as a control group. PTEN protein was decreased in the cardiac muscle from *Pten*^{l^p/l^p; *mck-Cre*^{+/-} mice compared with *Pten*^{l^p/l^p; *mck-Cre*^{-/-} mice (Fig. 6A). We also measured PTEN, p-Akt, and total Akt in these mice by Western blot analysis. PTEN was down-regulated in the heart and skeletal muscle from *Pten*^{l^p/l^p; *mck-Cre*^{+/-} mice, and p-Akt was increased in the heart but not in skeletal muscle (Fig. 6B). No difference was found in the liver from these mice. *Pten*^{l^p/l^p; *mck-Cre*^{+/-} mice developed cardiac hypertrophy (Fig. 6C). Importantly, MHC protein levels were increased in these mice (Fig. 6D).}}}}}}

3.7. LMP-2 deficiency leads to PTEN accumulation and cardiomyopathy

To determine whether LMP-2 downregulation is sufficient to induce PTEN accumulation, we measured PTEN protein levels in wildtype *Lmp-2*^{+/+} and *Lmp-2*^{-/-} hearts. In *Lmp-2*^{-/-} hearts, LMP-2 protein was undetectable (Fig. 7A); PTEN expression was significantly increased (Fig. 7A); p-Akt was significantly decreased (Fig. 7A). Furthermore, MHC protein levels were decreased in *Lmp-2*^{-/-} hearts (Fig. 7A). To determine whether LMP-2 is necessary for preservation of muscle mass and heart function, we measured left ventricular muscle mass (LVM) and FS in littermate *Lmp-2*^{+/+} and *Lmp-2*^{-/-} mice at the age of 18 months. LMP-2 deletion led to a balloon-like heart in mice (Fig. 7B). Despite increased heart weight in *Lmp-2*^{-/-} mice (0.221 vs 0.178 g), their LVM and FS were significantly decreased (Fig. 7C and 7D). Fibrotic tissue (white) was clearly seen in the endomyocardium of *Lmp-2*^{-/-} mice (Fig. 7C). Therefore, LMP-2 deficiency leads to loss of cardiac muscle mass and contractile dysfunction, a cardiomyopathy similar to that seen in type 2 diabetic hearts.

4. DISCUSSION

We have reported three important findings. First, we showed that high glucose increases LMP-7 and its respective chymotryptic-like proteasome activity and decreases LMP-2 in the heart. Second, we demonstrated that LMP-7 is up-regulated in STZ-induced diabetic hearts, and that increased chymotryptic-like proteasome activity contributes to the reduction of MHC protein levels. Third, we showed that LMP-2 is decreased in diabetic hearts, and that LMP-2 deficiency

leads to PTEN accumulation and Akt inactivation and results in cardiomyopathy in mice. Therefore, our study for the first time has demonstrated that immunoproteasome subunits play an important role in regulating cardiac muscle mass, and that their dysregulation may promote the development of diabetic cardiomyopathy.

Although immunoproteasome subunits are constitutively expressed in the heart, little is known about their regulation and function. Our knowledge about LMP-2 and LMP-7 largely comes from studies of inflammatory cells. LMP-2 and LMP-7 are encoded by the major histocompatibility complex class II region [22,23]. During infection, interferon- γ up-regulates LMP-2 and LMP-7 to promote antigen presentation [24]. Signal transducer and activator of transcription (Stat) 1 α and interferon regulatory factor 1 are required for their gene expression [25,26]. However, LMP-2 protein expression can be detected in *Stat-1* knockout mice under basal conditions [24]. A Stat-1-independent pathway may play an important role in regulating LMP-2 expression under non-inflammatory conditions. Nitric oxide up-regulates LMP-2 and LMP-7 protein levels through activation of cAMP-response element-binding protein [14]. In the present study, LMP-2 was decreased but LMP-7 was increased in STZ-induced diabetic hearts. We showed that high glucose decreases LMP-2 in the heart; therefore, hyperglycemia may contribute to the decrease in LMP-2 in diabetic hearts. Because LMP-2 can be downregulated by oxidants in the cell, the effect of high glucose on LMP-2 may be caused by increased ROS or decreased NO in diabetic hearts [27]. Although inflammatory factors in diabetic hearts have the potential to increase LMP-7 expression, LMP-7 is upregulated in isolated hearts exposed to high glucose, a condition in which inflammation is absent. Furthermore, STZ or high osmotic pressure did not have a direct impact on protein levels of the immunoproteasome subunits in perfused hearts. Therefore, high glucose may cause the differential regulation of LMP-2 and LMP-7 in the heart. This may help to explain why glycemic control is effective in preventing diabetic cardiomyopathy. It is not known whether hyperlipidemia and hypoinsulinemia also contribute to regulation of immunoproteasome subunits in diabetic hearts. Further studies are warranted to determine the molecular mechanisms responsible for the dysregulation of immunoproteasome subunits in diabetic hearts.

Muscle protein degradation is primarily mediated by chymotryptic-like proteasome activity [7]. LMP-7 protein levels are associated with the chymotryptic-like activity of 20S proteasomes [11,12,14]. Although constitutive β 5 subunit also mediates chymotryptic-like activity, it may not play an important role in determining this proteasome activity in the heart. It has been shown that increased chymotryptic-like activity is correlated with increased LMP-7 expression in the liver, and that relatively high β 5 subunit levels do not lead to high chymotryptic-like activity in the heart [12]. Importantly, LMP-7 over-expression leads to increased chymotryptic-like activity [28]. Consistent with the present study, a 68% increase in β 5 was found in diabetic hearts in a previous report by Powell et al [29]. However, this change is relatively modest compared with the 280% increase in LMP-7 we found in the diabetic hearts. Importantly, the high glucose-induced increase in chymotryptic-like activity was associated with upregulation of LMP-7, not the β 5 subunit. Moreover, no decrease in total protein synthesis was detected in STZ-induced diabetic hearts, and the loss of cardiac muscle mass resulted from increased proteasome activity, not from calcium-activated and lysosomal proteolysis [7]. The specific proteasome inhibitor EPX blocked loss of MHC protein by 75% in diabetic mice. EPX did not reduce blood glucose levels, but it had the same inhibitory effect on the development of diabetic cardiomyopathy as insulin. This suggests that EPX acts on the downstream target of high glucose. Therefore, our study indicates that 20S proteasome activation plays an important role in the development of diabetic cardiomyopathy. However, EPX and insulin did not fully prevent the loss of cardiac mass in diabetic mice despite the lack of a decrease in BW and cardiac function. Nevertheless, the fact that insulin was able to protect STZ mice against cardiomyopathy strongly suggests that the effects of STZ are largely independent of its

potential toxic effect on the heart. Since LMP-7 mediates chymotryptic-like activity, the upregulation of LMP-7, together with $\beta 5$ (at later time points), may increase proteolytic activity and promote degradation of cardiac muscle protein in STZ-induced diabetic mice. The loss of cardiac muscle mass mainly impairs systolic function and may not have an effect on diastolic function in these diabetic mice [30]. In the present study, LVEDP was not significantly changed in STZ mice, but the mice had a decrease in $-dp/dt$, suggesting that the relaxation in cardiac muscle was impaired.

In contrast to the STZ model, cardiomyopathy in the newly discovered type 1 diabetes model Akita mice is characterized by a loss in cardiac mass and diastolic function with preservation of systolic function [31]. However, Akita mice do not develop myocardial fibrosis [31]. Fibrosis is an important histopathological characteristic of diabetic cardiomyopathy, which has been implicated in the impairment of diastolic function in diabetes [32]. Thus, although Akita mice have the advantages of developing early onset of diastolic dysfunction and do not have potential extrapancreatic drug toxicity, these animals also have limitation with regard to extrapolation of findings to human diabetes [33]. Nevertheless, it will be interesting to determine whether the expression of LMP-7 and $\beta 5$ subunits in Akita mice is regulated in a similar manner as in STZ-treated mice.

LMP-2 plays an important role in the formation of immunoproteasomes. It has been reported that chymotryptic-like and tryptic-like proteasome activities are decreased in LMP-2 knockout mice [11,18]. Decreased tryptic-like proteasome activity in STZ-induced diabetic hearts supports the essential role of LMP-2 in assembling immunoproteasomes. However, it is not known why caspase-like proteasome activity, which is mediated by LMP-2, is increased in *Lmp-2^{-/-}* mice [11,18]. In our study, no change in caspase-like proteasome activity was found in STZ-induced diabetic mice, probably due to increased $\beta 1$ subunit in the heart. Interestingly, it has been proposed that LMP-2 can regulate the specificity of 20S proteasomes [34]. Indeed, LMP-2 deficiency causes the impairment of PTEN degradation in the heart [11]. Although PTEN may be one of many accumulated proteins, it plays an important role in cell growth, differentiation, and survival [35,36]. In cardiomyocytes, increased expression of PTEN causes myocyte atrophy by inactivating Akt [15]. The present study showed that muscle-specific PTEN inactivation increases cardiac muscle mass. Our findings therefore underscore the importance of PTEN in preserving cardiac muscle mass. In myocytes, Akt activity is regulated by PTEN and PI3K [7,35]. Activated Akt phosphorylates FOXO3a and increases its exportation from the nucleus to the cytoplasm, leading to decreased MAFbx expression [16, 17]. In STZ-induced diabetic hearts, the Akt/FOXO signaling pathway is regulated [7]. Our study further showed that MAFbx is increased in these diabetic hearts. MAFbx has been reported to inhibit myogenesis in skeletal muscle through degradation of MyoD1 [37]. Indeed, regeneration of cardiac muscle is impaired in STZ-induced diabetic mice [38]. Whether MyoD1 regulates myogenesis in the heart remains to be determined. Although the role of LMP-2 in regulating proteasome activity and specificity is not fully understood, LMP-2 deletion is sufficient to cause muscle mass loss and contractile dysfunction in the heart. LMP-7 upregulation may have an additive effect on the process by increasing muscle protein degradation.

In conclusion, high glucose upregulates LMP-7 and its corresponding chymotryptic-like proteasome activity and downregulates LMP-2 in the heart. The dysregulation of immunoproteasome subunits is present in STZ-induced diabetic hearts, leading to UPS dysfunction and loss of cardiac muscle mass. Our study suggests that immunoproteasome subunits play a critical role in regulating cardiac muscle mass under physiological and pathological conditions. Therefore, immunoproteasome subunits may be effective therapeutic targets for preventing and treating diabetic cardiomyopathy.

Supplementary Material

Refer to Web version on PubMed Central for supplementary material.

Acknowledgments

This work was supported by Public Health Service grant P01-HL65608 (to L.C.B) and HL88071 (to Z.P.C) from the National Heart, Lung and Blood Institute, National Institutes of Health.

References

1. Ho KK, Pinsky JL, Kannel WB, Levy D. The epidemiology of heart failure: the Framingham Study. *J Am Coll Cardiol* 1993;22:6A–13A. [PubMed: 8509564]
2. Kannel WB, Hjortland M, Castelli WP. Role of diabetes in congestive heart failure: the Framingham study. *Am J Cardiol* 1974;34:29–34. [PubMed: 4835750]
3. Jackson CV, McGrath GM, Tahiliani AG, Vadlamudi RV, McNeill JH. A functional and ultrastructural analysis of experimental diabetic rat myocardium. Manifestation of a cardiomyopathy. *Diabetes* 1985;34:876–883. [PubMed: 3896897]
4. Aneja A, Tang WH, Bansilal S, Garcia MJ, Farkouh ME. Diabetic cardiomyopathy: insights into pathogenesis, diagnostic challenges, and therapeutic options. *Am J Med* 2008;121:748–57. [PubMed: 18724960]
5. Kettelhut IC, Pepato MT, Migliorini RH, Medina R, Goldberg AL. Regulation of different proteolytic pathways in skeletal muscle in fasting and diabetes mellitus. *Braz J Med Biol Res* 1994;27:981–93. [PubMed: 8087098]
6. Merforth S, Osmers A, Dahlmann B. Alterations of proteasome activities in skeletal muscle tissue of diabetic rats. *Mol Biol Rep* 1999;26:83–7. [PubMed: 10363652]
7. Hu J, Klein JD, Du J, Wang XH. Cardiac muscle protein catabolism in diabetes mellitus: activation of the ubiquitin-proteasome system by insulin deficiency. *Endocrinology* 2008;149:5384–5390. [PubMed: 18653708]
8. Willis MS, Patterson C. Into the heart: the emerging role of the ubiquitin-proteasome system. *J Mol Cell Cardiol* 2006;41:567–579. [PubMed: 16949602]
9. Gillette TG, Kumar B, Thompson D, Slaughter CA, DeMartino GN. Differential roles of the COOH termini of AAA subunits of PA700 (19 S regulator) in asymmetric assembly and activation of the 26 S proteasome. *J Biol Chem* 2008;283:31813–31822. [PubMed: 18796432]
10. Rabl J, Smith DM, Yu Y, Chang SC, Goldberg AL, Cheng Y. Mechanism of gate opening in the 20S proteasome by the proteasomal ATPases. *Mol Cell* 2008;30:360–8. [PubMed: 18471981]
11. Cai ZP, Shen Z, Van Kaer L, Becker LC. Ischemic preconditioning-induced cardioprotection is lost in mice with immunoproteasome subunit low molecular mass polypeptide-2 deficiency. *FASEB J* 2008;22:4248–4257. [PubMed: 18728217]
12. Gomes AV, Young GW, Wang Y, Zong C, Eghbali M, Drews O, et al. Contrasting proteome biology and functional heterogeneity of the 20 S proteasome complexes in mammalian tissues. *Mol Cell Proteomics* 2009;8:302–315. [PubMed: 18931337]
13. Griffin TA, Nandi D, Cruz M, Fehling HJ, Kaer LV, Monaco JJ, et al. Immunoproteasome assembly: cooperative incorporation of interferon gamma (IFN-gamma)-inducible subunits. *J Exp Med* 1998;187:97–104. [PubMed: 9419215]
14. Kotamraju S, Matalon S, Matsunaga T, Shang T, Hickman-Davis JM, Kalyanaraman B. Upregulation of immunoproteasomes by nitric oxide: potential antioxidative mechanism in endothelial cells. *Free Radic Biol Med* 2006;40:1034–1044. [PubMed: 16540399]
15. Schwartzbauer G, Robbins J. The tumor suppressor gene PTEN can regulate cardiac hypertrophy and survival. *J Biol Chem* 2001;276:35786–35793. [PubMed: 11448956]
16. Skurk C, Izumiya Y, Maatz H, Razeghi P, Shiojima I, Sandri M, et al. The FOXO3a transcription factor regulates cardiac myocyte size downstream of AKT signaling. *J Biol Chem* 2005;280:20814–20823. [PubMed: 15781459]

17. Sandri M, Sandri C, Gilbert A, Skurk C, Calabria E, Picard A, et al. Foxo transcription factors induce the atrophy-related ubiquitin ligase atrogin-1 and cause skeletal muscle atrophy. *Cell* 2004;117:399–412. [PubMed: 15109499]
18. Van Kaer L, Ashton-Rickardt PG, Eichelberger M, Gaczynska M, Nagashima K, Rock KL, et al. Altered peptidase and viral-specific T cell response in LMP2 mutant mice. *Immunity* 1994;1:533–541. [PubMed: 7600282]
19. Hedhli N, Lizano P, Hong C, Fritzky LF, Dhar SK, Liu H, et al. Proteasome inhibition decreases cardiac remodeling after initiation of pressure overload. *Am J Physiol Heart Circ Physiol* 2008;295:H1385–93. [PubMed: 18676687]
20. Cai Z, Zhong H, Bosch-Marce M, Fox-Talbot K, Wang L, Wei C, et al. Complete loss of ischaemic preconditioning-induced cardioprotection in mice with partial deficiency of HIF-1 alpha. *Cardiovasc Res* 2008;77:463–70. [PubMed: 18006459]
21. Koitabashi N, Bedja D, Zaiman AL, Pinto YM, Zhang M, Gabrielson KL, et al. Avoidance of transient cardiomyopathy in cardiomyocyte-targeted tamoxifen-induced MerCreMer gene deletion models. *Circ Res* 2009;105:12–5. [PubMed: 19520971]
22. Martinez CK, Monaco JJ. Homology of proteasome subunits to a major histocompatibility complex-linked LMP gene. *Nature* 1991;353:664–7. [PubMed: 1681432]
23. Glynne R, Powis SH, Beck S, Kelly A, Kerr LA, Trowsdale J. A proteasome-related gene between the two ABC transporter loci in the class II region of the human MHC. *Nature* 1991;353:357–360. [PubMed: 1922342]
24. Barton LF, Cruz M, Rangwala R, Deepe GS Jr, Monaco JJ. Regulation of immunoproteasome subunit expression in vivo following pathogenic fungal infection. *J Immunol* 2002;169:3046–3052. [PubMed: 12218120]
25. Chatterjee-Kishore M, Kishore R, Hicklin DJ, Marincola FM, Ferrone S. Different requirements for signal transducer and activator of transcription 1alpha and interferon regulatory factor 1 in the regulation of low molecular mass polypeptide 2 and transporter associated with antigen processing 1 gene expression. *J Biol Chem* 1998;273:16177–16183. [PubMed: 9632673]
26. Chatterjee-Kishore M, Wright KL, Ting JP, Stark GR. How Stat1 mediates constitutive gene expression: a complex of unphosphorylated Stat1 and IRF1 supports transcription of the LMP2 gene. *EMBO J* 2000;19:4111–4122. [PubMed: 10921891]
27. Khan MA, Oubrahim H, Stadtman ER. Inhibition of apoptosis in acute promyelocytic leukemia cells leads to increases in levels of oxidized protein and LMP2 immunoproteasome. *Proc Natl Acad Sci USA* 2004;101:11560–11565. [PubMed: 15284441]
28. Gaczynska M, Rock KL, Spies T, Goldberg AL. Peptidase activities of proteasomes are differentially regulated by the major histocompatibility complex-encoded genes for LMP2 and LMP7. *Proc Natl Acad Sci USA* 1994;91:9213–9217. [PubMed: 7937744]
29. Powell SR, Samuel SM, Wang P, Divald A, Thirunavukkarasu M, Koneru S, et al. Upregulation of myocardial 11S-activated proteasome in experimental hyperglycemia. *J Mol Cell Cardiol* 2008;44:618–621. [PubMed: 18308332]
30. Harris IS, Treskov I, Rowley MW, Heximer S, Kaltenbronn K, Finck BN, et al. G-protein signaling participates in the development of diabetic cardiomyopathy. *Diabetes* 2004;53:3082–90. [PubMed: 15561937]
31. Basu R, Oudit GY, Wang X, Zhang L, Ussher JR, Lopaschuk GD, et al. Type 1 diabetic cardiomyopathy in the Akita (Ins2WT/C96Y) mouse model is characterized by lipotoxicity and diastolic dysfunction with preserved systolic function. *Am J Physiol Heart Circ Physiol* 2009;297:H2096–108. [PubMed: 19801494]
32. Fang ZY, Prins JB, Marwick TH. Diabetic cardiomyopathy: evidence, mechanisms, and therapeutic implications. *Endocr Rev* 2004;25:543–67. [PubMed: 15294881]
33. Bugger H, Abel ED. Rodent models of diabetic cardiomyopathy. *Dis Model Mech* 2009;2:454–66. [PubMed: 19726805]
34. Sijts AJ, Ruppert T, Rehmann B, Schmidt M, Koszinowski U, Kloetzel PM. Efficient generation of a hepatitis B virus cytotoxic T lymphocyte epitope requires the structural features of immunoproteasomes. *J Exp Med* 2000;191:503–514. [PubMed: 10662796]

35. Crackower MA, Oudit GY, Kozieradzki I, Sarao R, Sun H, Sasaki T, et al. Regulation of myocardial contractility and cell size by distinct PI3K-PTEN signaling pathways. *Cell* 2002;110:737–49. [PubMed: 12297047]
36. Oudit GY, Kassiri Z, Zhou J, Liu QC, Liu PP, Backx PH, et al. Loss of PTEN attenuates the development of pathological hypertrophy and heart failure in response to biomechanical stress. *Cardiovasc Res* 2008;78:505–14. [PubMed: 18281373]
37. Lagirand-Cantaloube J, Cornille K, Csibi A, Batonnet-Pichon S, Leibovitch MP, Leibovitch SA. Inhibition of atrogenin-1/MAFbx mediated MyoD proteolysis prevents skeletal muscle atrophy in vivo. *PLoS One* 2009;4:e4973. [PubMed: 19319192]
38. Rota M, LeCapitaine N, Hosoda T, Boni A, De Angelis A, Padin-Iruegas ME, et al. Diabetes promotes cardiac stem cell aging and heart failure, which are prevented by deletion of the p66shc gene. *Circ Res* 2006;99:42–52. [PubMed: 16763167]

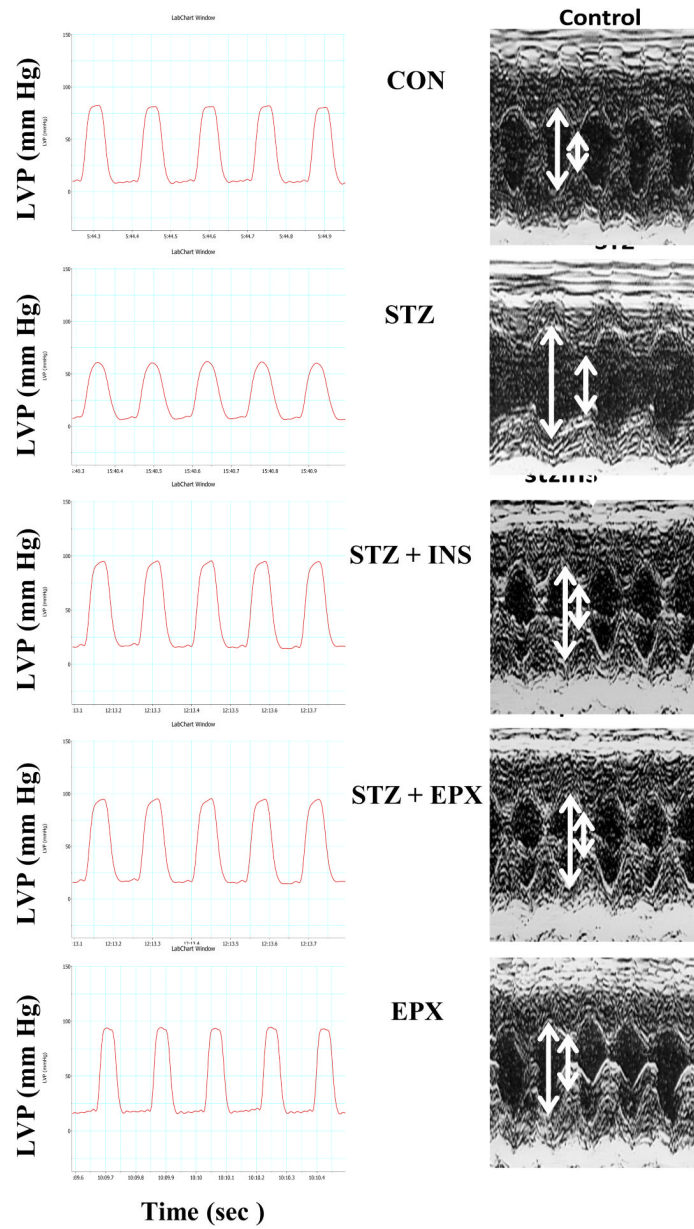


FIG. 1. Diabetic cardiomyopathy is attenuated by EPX in STZ mice. Diabetes was induced in wildtype C57BL6 mice with STZ. Insulin and epoxomicin (EPX) were used to treat diabetic mice for 6 weeks. Vehicle (CON) and EPX only treatment were controls. Representative left ventricular pressure recording and echocardiography. Each picture was chosen from 4–5 animal studies.

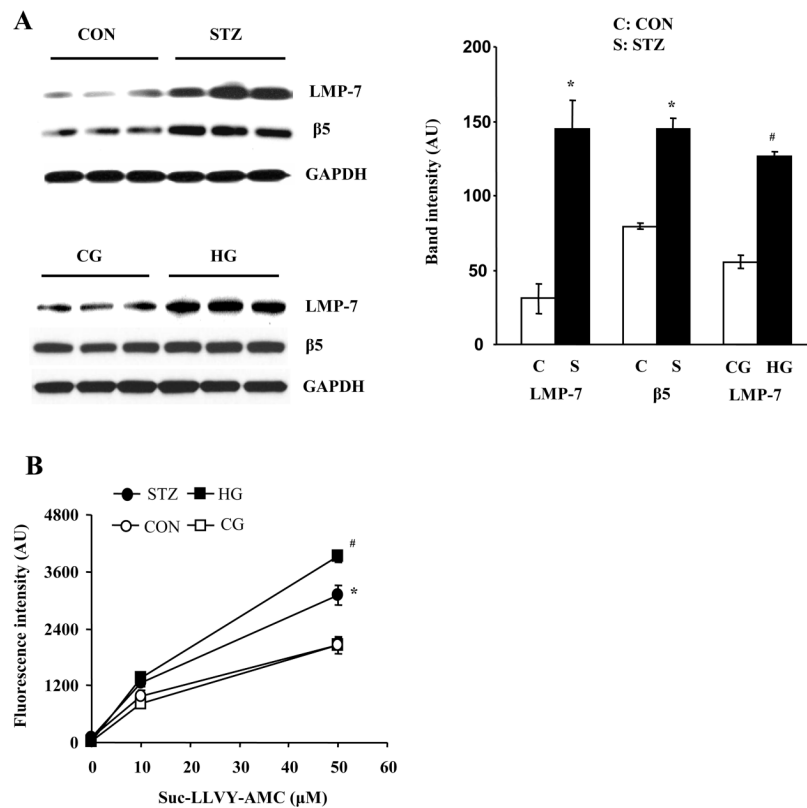
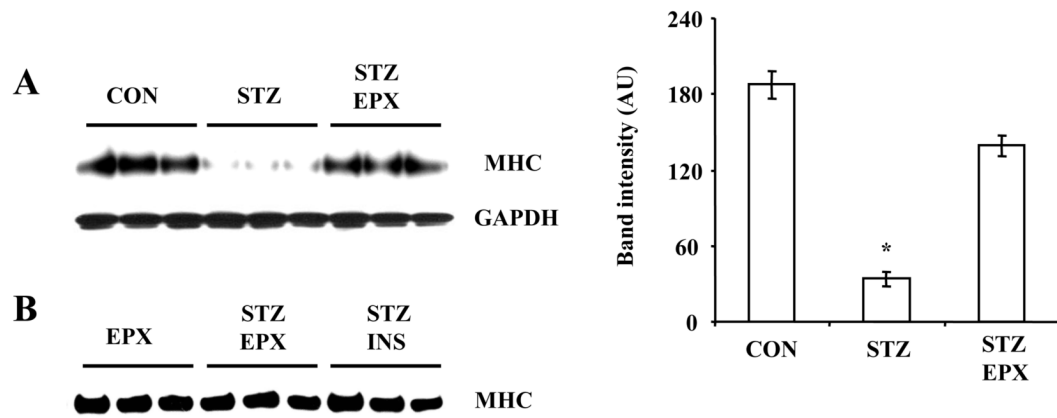


FIG. 2. LMP-7 is up-regulated and chymotryptic-like proteasome activity is increased in STZ-induced diabetic hearts and normal hearts treated with high glucose. **A:** STZ (S) and CON (C) hearts were collected for Western blot analysis of LMP-7 and β5 subunit. GAPDH was used as a loading control. Isolated hearts from wildtype mice were exposed to high glucose (HG) and control glucose (CG) for 4 hrs. LMP-7 and β5 subunit protein levels were examined. **B:** Chymotryptic-like proteasome activity was measured by fluorogenic assay in STZ and CON hearts and in HG and CG hearts (D). N = 3–4. *: p < 0.01 vs. CON. #: p < 0.01 vs. CG.

**FIG. 3.**

MHC protein levels are reduced in STZ-induced diabetic hearts and this is inhibited by EPX. Diabetic mice were treated with or without EPX for 6 weeks. MHC was analyzed by Western blot analysis. N = 3, *: $p < 0.01$ vs. CON or EPX. B: Diabetic mice were treated with EPX or insulin and normal mice were treated with EPX for 6 weeks.

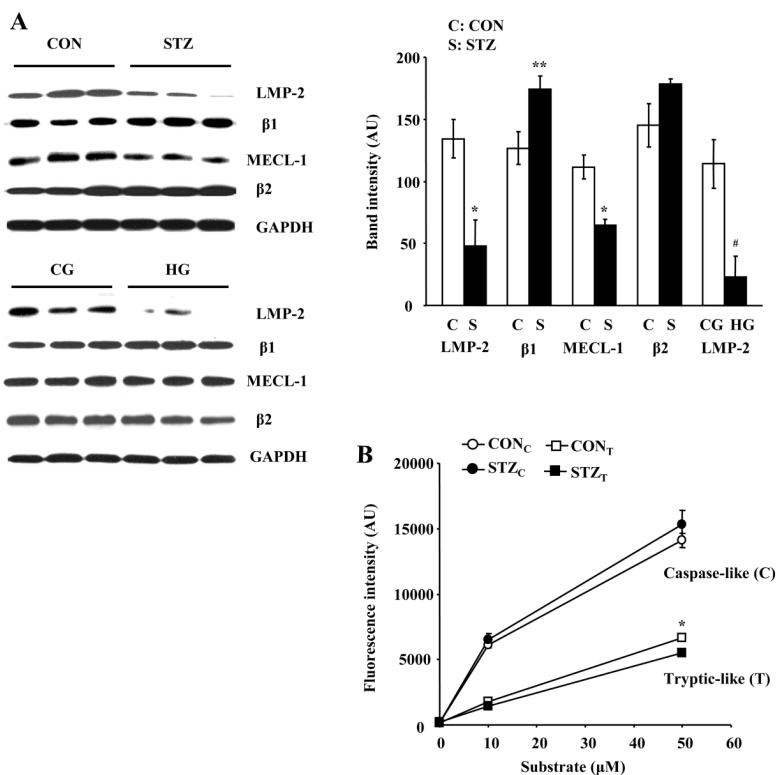


FIG. 4. LMP-2 and MECL-1 protein levels and tryptic-like proteasome activity are decreased in STZ-induced diabetic hearts. A: LMP-2, β 1, MECL-1, and β 2 were measured by Western blot analysis in STZ (S, solid bar) and CON (C, open bar) hearts and in HG and CG hearts. B: Tryptic-like and caspase-like proteasome activities were measured in STZ and CON hearts. N = 3–4, *: p < 0.01 vs. CON. **: p < 0.05 vs. CON. #: p < 0.01 vs. CG.

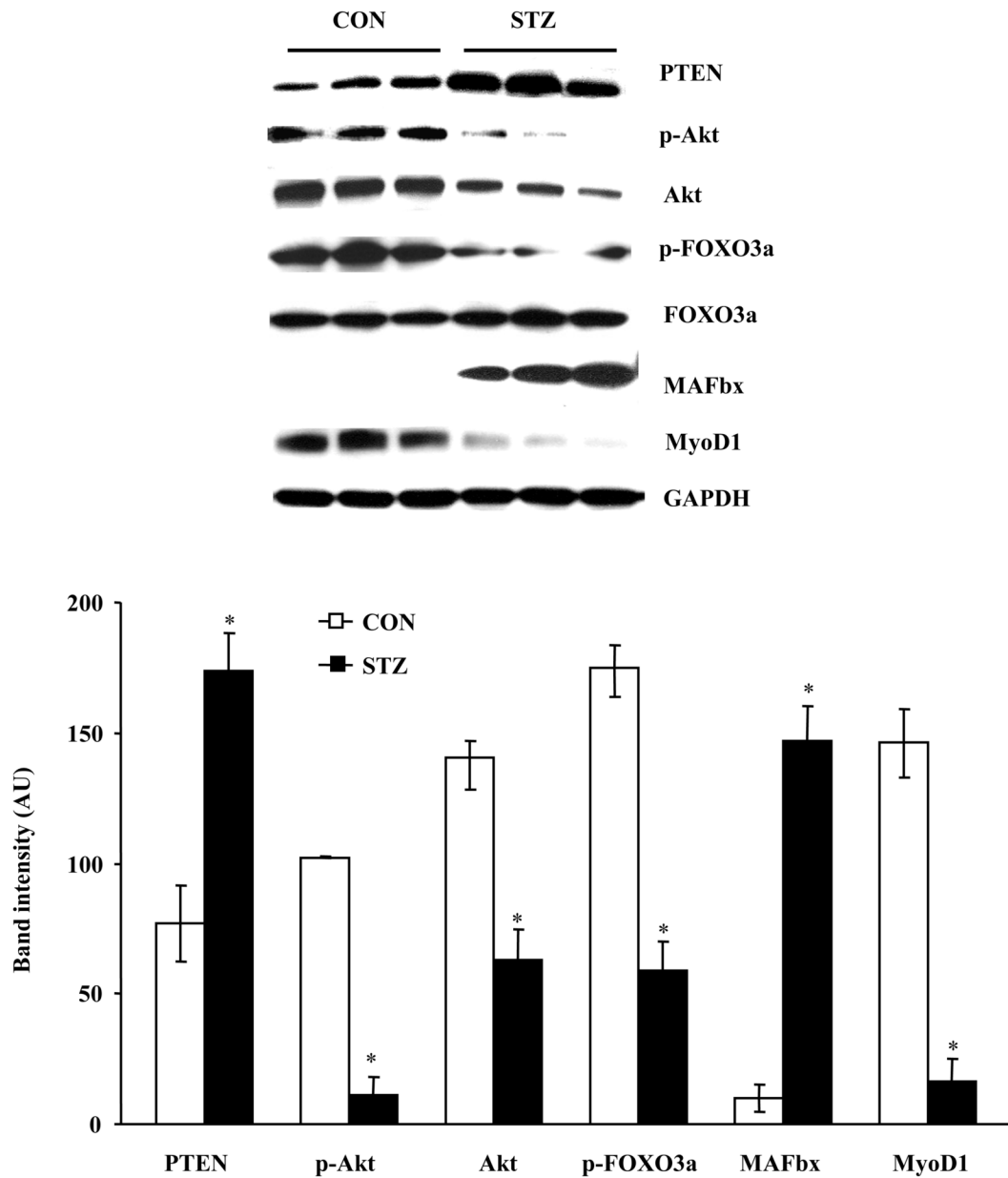
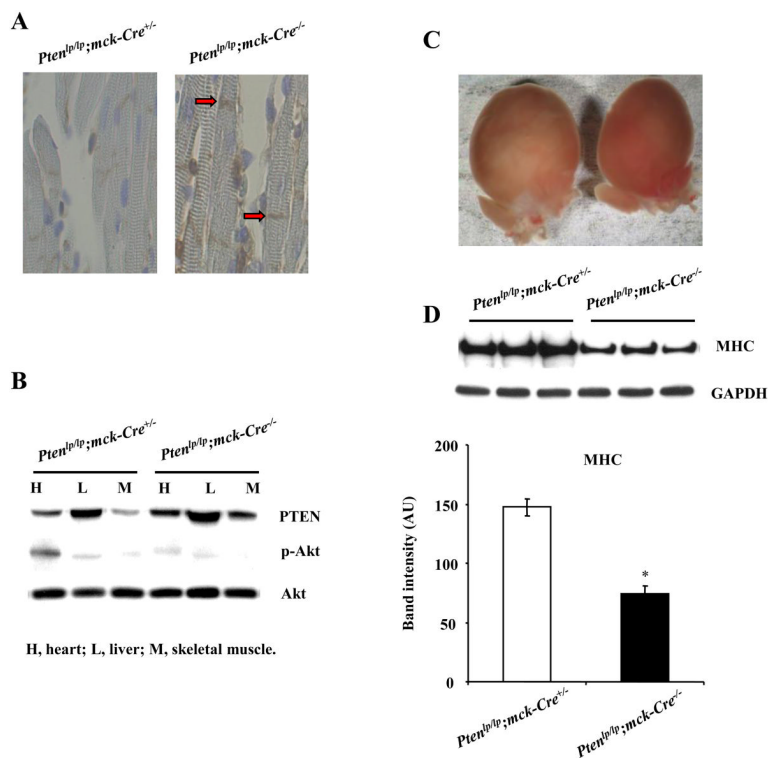
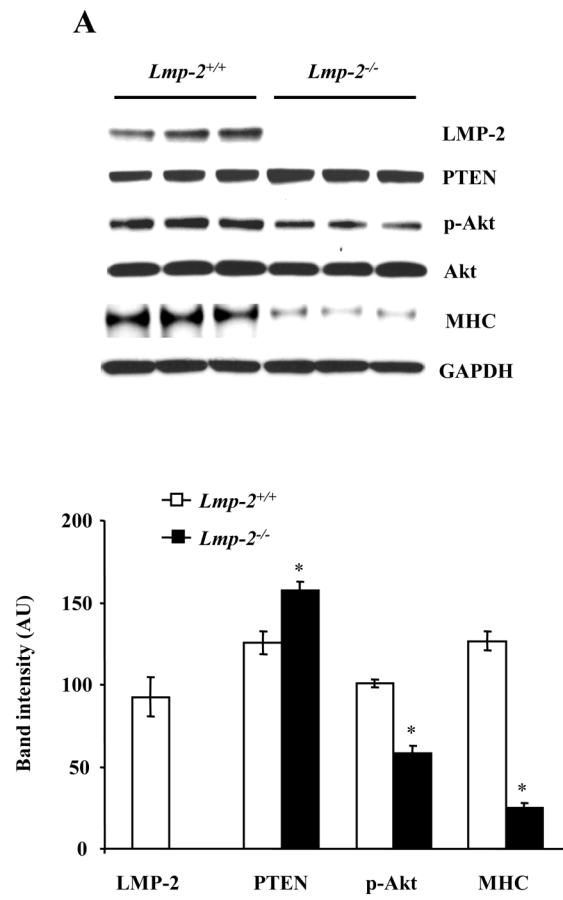


FIG. 5. PTEN/Akt/FOXO3a/MAFbx signaling axis is regulated in STZ-induced diabetic hearts. PTEN, p-Akt and Akt, p-FOXO3a and FOXO3a, MAFbx, and MyoD1 were analyzed in STZ (S, solid bar) and CON (C, open bar) hearts. N = 3, *: p < 0.01 vs. CON.

**FIG. 6.**

Cardiac muscle mass is increased in muscle-specific *Pten* knockout mice. A: PTEN immunohistochemistry. PTEN was expressed in cardiac muscle in *Pten^{lp/lp}; mck-Cre^{+/+}* control mice (red arrows), but undetectable in *Pten^{lp/lp}; mck-Cre^{-/-}* control mice. B: PTEN, p-Akt, and total Akt protein levels in the heart, liver, and skeletal muscle. C: Whole hearts of *Pten* control and knockout mice. The data from A–C are representative of 3 *Pten^{lp/lp}; mck-Cre^{+/+}* mice and 3 *Pten^{lp/lp}; mck-Cre^{-/-}* mice. D: MHC was increased in *Pten^{lp/lp}; mck-Cre^{+/+}* mice. N = 3, *: p < 0.01 vs. *Pten^{lp/lp}; mck-Cre^{-/-}*.



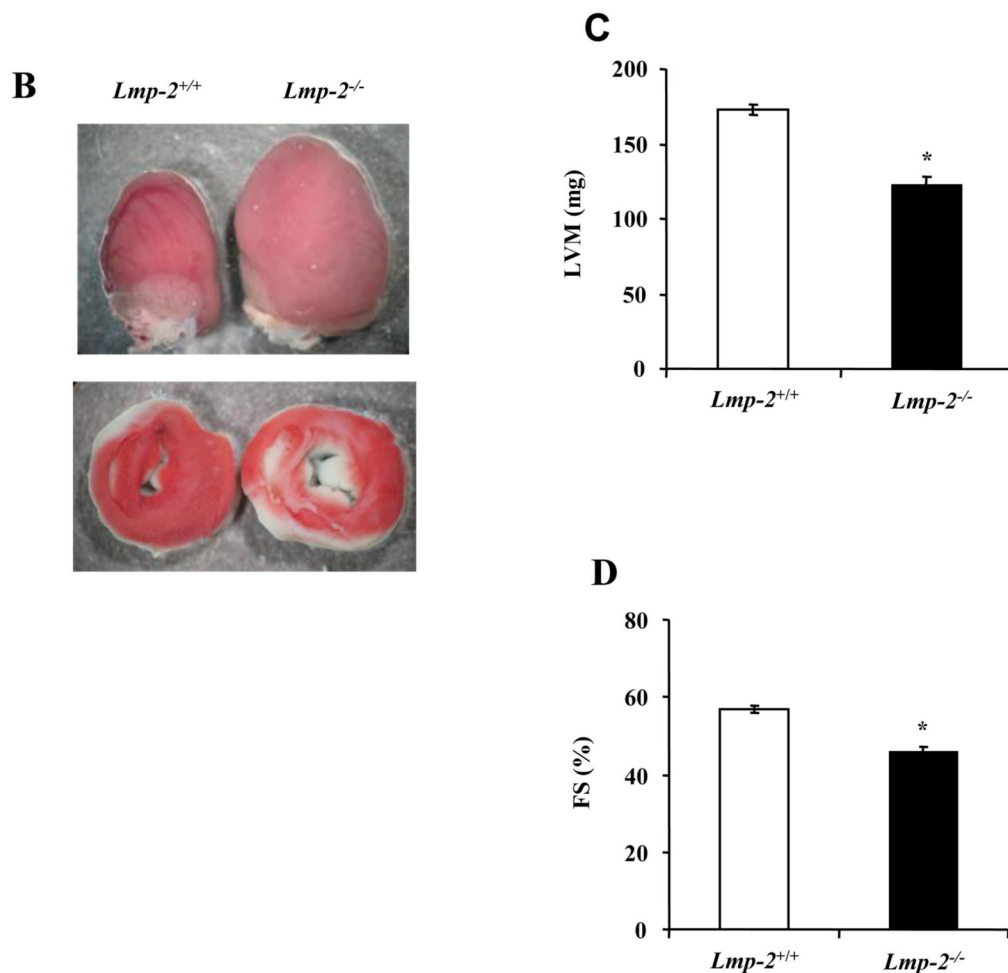


FIG. 7. LMP-2 deficiency leads to loss of cardiac muscle mass and a decrease in cardiac function in mice. A: Western blots of LMP-2, PTEN, p-Akt and Akt, and MHC in *Lmp-2^{+/+}* (open bar) and *Lmp-2^{-/-}* (solid bar) mice. N = 4, *: p < 0.05 vs. *Lmp-2^{+/+}*. B: Whole hearts and middle sections from *Lmp-2^{+/+}* and *Lmp-2^{-/-}* mice. The thickness of left ventricular muscle (red) was decreased. Fibrotic tissue (white) formed in the endomyocardium. The pictures are representative of 4 *Lmp-2^{+/+}* mice and 4 *Lmp-2^{-/-}* mice. C and D: LVM and FS were decreased in *Lmp-2^{-/-}* mice. N = 4, *: p < 0.01 vs. *Lmp-2^{+/+}*.

Table 1

Ventricular parameter in 14-week-old mice

	CON n = 10	STZ n = 10	STZ + INS n = 5	STZ + EPX n = 7	EPX n = 4
GLU, mg/dl	S 110 ± 4	418 ± 16 ^a	398 ± 52	408 ± 33	116 ± 3
	E 108 ± 3	547 ± 27 ^a	156 ± 11	533 ± 31	120 ± 6
BW, g	27.9 ± 0.7	20.1 ± 1.0 ^a	25.7 ± 1.1 ^c	24.0 ± 0.6 ^d	27.5 ± 0.7
HW, mg	139.4 ± 3.6	103.3 ± 3.0 ^a	117.6 ± 3.8 ^{a,d}	115.0 ± 3.3 ^{a,d}	124.7 ± 6.3
TL, mm	2.12 ± 0.02	2.08 ± 0.02	2.10 ± 0.02	2.08 ± 0.02	2.08 ± 0.02
HW/TL, mg/mm	65.7 ± 1.7	49.7 ± 1.4 ^a	56.0 ± 2.0 ^{a,d}	54.3 ± 1.6 ^{a,d}	59.9 ± 3.0
HW/BW, mg/g	4.99 ± 0.06	4.88 ± 0.14	4.59 ± 0.12 ^a	4.71 ± 0.18	4.53 ± 0.12 ^a
HR, bpm	447 ± 14	468 ± 14	446 ± 21	519 ± 27	467 ± 58
LVDP, mm Hg	75 ± 3	56 ± 5.5 ^a	84 ± 4 ^c	84 ± 3 ^c	90 ± 7
LVEDP, mm Hg	10 ± 1	8 ± 1	14 ± 2	11 ± 2	10 ± 2
(+)dp/dt, mm Hg/sec	4270 ± 230	2716 ± 470 ^b	4118 ± 21 ^d	3908 ± 281	5158 ± 350
(-)dp/dt, mm Hg/sec	3783 ± 191	2095 ± 405 ^a	3862 ± 321 ^d	3807 ± 156 ^d	5147 ± 825
EDD, mm	2.92 ± 0.07	2.67 ± 0.03 ^b	2.92 ± 0.08	2.88 ± 0.10	2.95 ± 0.10
ESD, mm	1.15 ± 0.04	1.53 ± 0.08 ^a	1.04 ± 0.04 ^d	1.18 ± 0.07	1.18 ± 0.04
FS, %	60.6 ± 0.6	42.5 ± 3.2 ^a	64.4 ± 0.6 ^c	59.2 ± 1.3 ^c	60.1 ± 0.6

Type 1 diabetes was induced by STZ. Insulin (INS) and epoxomicin (EPX) were used to treat diabetic mice for 6 weeks. Blood glucose (GLU) was measured at the start (S) of the treatments and at the end (E) of the experiment. BW, body weight; HW, heart weight; TL, tibial length; HR, heart rate; LVDP, left ventricular developed pressure; EDD, end-diastolic diameter; ESD, end-systolic diameter; FS, fractional shortening.

^a p < 0.01 vs CON.

^b p < 0.05 vs CON.

^c p < 0.01 vs STZ.

^d p < 0.05 vs STZ.